The Madden–Julian Oscillation, Barotropic Dynamics, and North Pacific Tropical Cyclone Formation. Part I: Observations

ERIC D. MALONEY AND DENNIS L. HARTMANN

Department of Atmospheric Sciences, University of Washington, Seattle, Washington

(Manuscript received 20 September 2000, in final form 9 February 2001)

ABSTRACT

Low-level barotropic dynamics may help to explain the modulation of eastern and western North Pacific tropical cyclones by the Madden–Julian oscillation (MJO) during Northern Hemisphere summer. The MJO is characterized by alternating periods of westerly and easterly 850-mb zonal wind anomalies across the tropical Pacific Ocean. When MJO 850-mb wind anomalies are westerly, small-scale, slow-moving eddies grow through barotropic eddy kinetic energy (EKE) conversion from the mean flow. These growing eddies, together with strong surface convergence, 850-mb cyclonic shear, and high mean sea surface temperatures, create a favorable environment for tropical cyclone formation. Periods of strong MJO easterlies over the Pacific are characterized by lesser EKE and negligible eddy growth by barotropic conversion.

The term $-\overline{u'^2}\partial\overline{u}/\partial x$ is a leading contributor to low-level barotropic EKE conversion during MJO westerly periods across the Pacific, indicating the importance of zonal variations in the westerly jet for producing concentrations of eddy energy. This mechanism can be described as wave accumulation associated with variations of the low-level zonal flow. The conversion term $-\overline{u'v'}\partial\overline{u}/\partial y$ contributes a smaller portion of the total conversion over the eastern Pacific, but is of comparable importance to $-\overline{u'^2}\partial\overline{u}/\partial x$ during westerly MJO events in the western Pacific.

1. Introduction

Barotropic dynamics have been shown to be important to the formation and growth of wave disturbances from which tropical cyclones evolve. For example, African easterly waves over the tropical Atlantic are maintained by barotropic energy conversions from the mean flow (Norquist et al. 1977). Barotropic conversions may also be crucial to the formation of the most unstable easterly waves near the African easterly jet (Thorncroft and Hoskins 1994a), although baroclinic conversions do contribute to wave intensification (Thorncroft and Hoskins 1994b). As these African easterly waves travel into the Caribbean Sea, barotropic instability at lower levels may intensify the waves, providing energetic precursor disturbances for eastern Pacific and Caribbean tropical cyclones (Molinari et al. 1997; Molinari and Vollaro 2000). Schubert et al. (1991) and Nieto Ferreira and Schubert (1997) suggest that the eastern Pacific intertropical convergence zone may occasionally break down into multiple tropical disturbances through barotropic instability in the lower troposphere. This local unstable wave growth supports tropical cyclogenesis over the eastern Pacific Ocean. Although latent heat release and baroclinic processes clearly play a key role in mature tropical cyclones, previous observational studies have found that developing tropical depressions are often barotropic to first order (e.g., Shapiro 1978; Davidson and Hendon 1989).

Tropical wave disturbances can also amplify through barotropic wave accumulation by the mean flow. Barotropic Rossby wave accumulation through convergence of the low-level zonal flow contributes to the growth of tropical depression-type disturbances over the western Pacific (Webster and Chang 1988; Holland 1995; Sobel and Bretherton 1999). Western Pacific barotropic wave accumulation may be enhanced during active periods of the Madden–Julian oscillation (MJO; Sobel and Maloney 2000). Equatorial western Pacific mixed-Rossby gravity waves are characterized by decreased phase speed and wavelength, and increased amplitude during periods of wave accumulation associated with MJO low-level convergence (Dickinson 2000). See Madden and Julian (1994) for a thorough review of the MJO.

In this paper, we examine the importance of barotropic dynamics to eddy kinetic energy growth in tropical cyclone formation regions during MJO westerly events in the North Pacific Ocean. We will consider the eastern North Pacific and western North Pacific tropical cyclone genesis regions. The MJO is characterized by alternating periods of easterly and westerly zonal wind

Corresponding author address: Eric Maloney, NCAR/CGD, P. O. Box 3000, Boulder, CO 80307-3000.
E-mail: maloney@ucar.edu

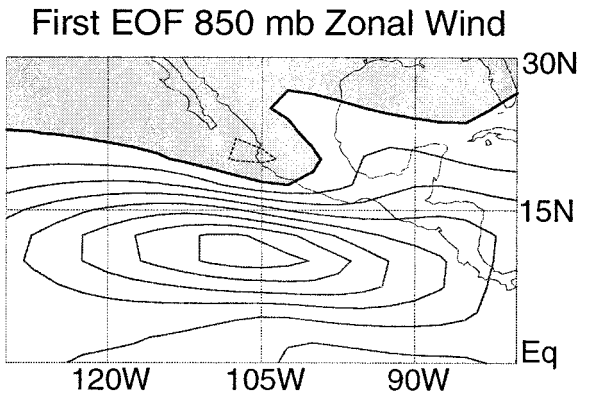

FIG. 1. Leading EOF of the 850-mb zonal wind for May–Nov 1979–97, equator–30°N, 80°–130°W. Negative values are shaded. Contours are evenly spaced at 0.02. Magnitudes are normalized.

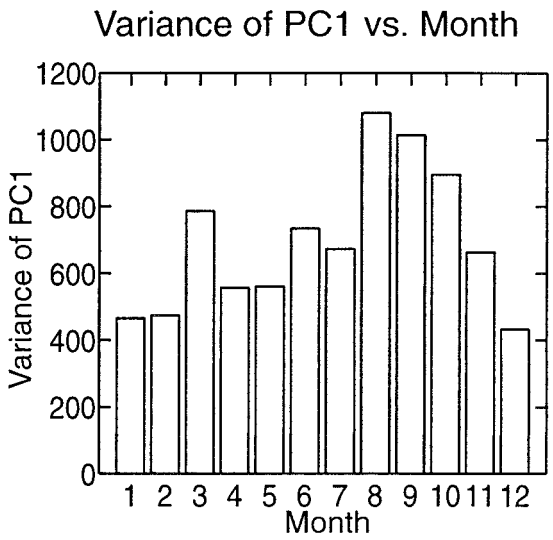

FIG. 2. Variance of the first principal component as a function of month (units: $m^2\ s^{-2}$).

anomalies across the tropical Pacific Ocean during Northern Hemisphere summer (Maloney and Hartmann 2000a, hereafter MH00). We hypothesize that barotropic energy conversions (e.g., Hoskins et al. 1983; Mak and Cai 1989) provide a significant source of eddy kinetic energy during westerly MJO periods, and that these growing eddies provide seed disturbances that may develop into tropical cyclones when other environmental conditions are favorable. Cyclonic low-level relative vorticity, low-level convergence, and weak vertical wind shear provide a favorable environment for tropical cyclone genesis (Zehr 1992; Gray 1998), and these conditions are prevalent during MJO westerly periods (MH00). We particularly focus on the low-level flow, since MH00 found that the 850-mb wind anomaly field varies more strongly than the 200-mb field over the eastern Pacific hurricane region during an MJO composite life cycle. The barotropic conversion mechanism we discuss in this paper will prove to be consistent with the 850-mb barotropic wave-accumulation arguments of Sobel and Bretherton (1999) and Sobel and Maloney (2000).

This paper does not claim that low-level barotropic dynamics can explain all aspects of tropical cyclone formation across the Pacific basin. Latent heat release is clearly important to developing and mature tropical cyclones, and mature tropical cyclones are characterized by strong vertical shears away from the center. Upper-level vorticity features can also influence the development of tropical cyclones (e.g., Montgomery and Farrell 1993), and high sea surface temperatures are a necessary condition for tropical cyclone development (Emanuel 1988; Gray 1998). We will show, however, that lower tropospheric barotropic dynamics can provide a significant source of kinetic energy for tropical wave disturbances during MJO westerly periods.

This paper is organized as follows. Section 3 determines the mode of variability in the 850-mb zonal winds over the eastern Pacific during May–November that characterizes the MJO. Periods of high amplitude of this mode will be averaged to produce composite events. Composites will define periods of strong westerly jets or enhanced easterly winds over the eastern Pacific Ocean, which vary at intraseasonal timescales. MH00 found that eastern Pacific hurricanes are four times more likely during MJO westerly periods than easterly periods. Eastern Pacific eddy kinetic energy during westerly and easterly periods will be diagnosed, and the rate of barotropic energy conversion from the mean state to eddies will be determined. The spatial structure and amplitude of the dominant eddies will be analyzed for westerly wind periods. We will examine whether local barotropic dynamics can be sufficient to foster wave growth and seed hurricane formation over the eastern Pacific. Section 4 will describe a similar analysis for the western Pacific Ocean, where Liebmann et al. (1994) documented a modulation of tropical cyclone activity by the MJO. Conclusions will follow in section 5. Hartmann and Maloney (2001, Part II of this study), examine eddy behavior over the Pacific Ocean during an MJO life cycle using a stochastically forced 2D barotropic model.

2. Data

The National Centers for Environmental Prediction–National Center for Atmospheric Research (NCEP–NCAR) gridded reanalysis wind product (Kalnay et al. 1996) in pentad format (2.5° by 2.5°) is used at 850 and 1000 mb for 1979–97. The annual cycle is removed from the time series when appropriate. The annual cycle is determined by calculating pentad means for the entire time series and then smoothing with a 1-2-1 filter. Daily data, recorded once daily at 0000 UTC were used during times of significant events for better resolution in calculating eddy statistics. Our results are subject to the assumption that the NCEP reanalysis product produces

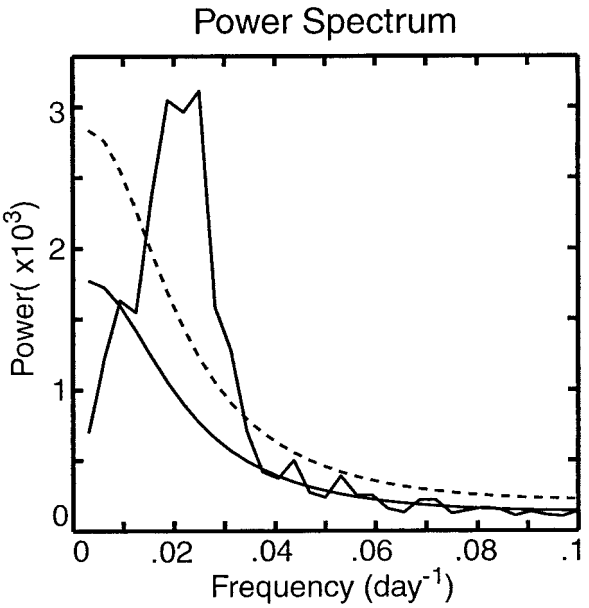

FIG. 3. Average power spectrum of the first principal component, computed for 64 pentad periods centered on Aug of each year during 1979–97. The red noise spectrum is displayed along with the a priori 95% confidence limit (dashed).

realistic winds over the Pacific. The Advanced Very High Resolution Radiometer National Oceanic and Atmospheric Administration outgoing longwave radiation (OLR) product (Gruber and Krueger 1984) during 1979–97 is used in the composite analysis.

3. Eastern Pacific energetics

The goal of this section is to examine the role of MJO wind variations in focusing wave activity in regions where eastern Pacific tropical cyclones form. We will develop a local MJO index based on empirical orthogonal function (EOF) analysis of the eastern Pacific 850-mb zonal wind. We will then examine the role of the MJO in concentrating eddy activity through barotropic dynamics over the eastern Pacific hurricane region. Figure 1 of MH00 describes the eastern Pacific tropical cyclone genesis region.

a. EOF analysis

We now use EOF analysis to determine the dominant mode of zonal wind variability over the eastern Pacific during the hurricane season. EOF analysis is conducted on the 850-mb zonal wind time series during 1979–97 in the region 0°–30°N, 75°–125°W for May–November. The annual cycle is first removed from the data. The first EOF, which explains 38% of the variance, is shown in Fig. 1. The second and third EOFs explain 10% and 8% of the variance, respectively. The leading EOF is significantly different from the rest based on the criterion developed by North et al. (1982). The first EOF depicts a jetlike zonal wind structure centered at about 10°N. The location of this jet is consistent with the location of maximum wind anomalies over the eastern Pacific in the MJO composites of MH00. EOF analysis on an expanded region (not shown) shows this jet to be in phase with equatorial wind anomalies westward to

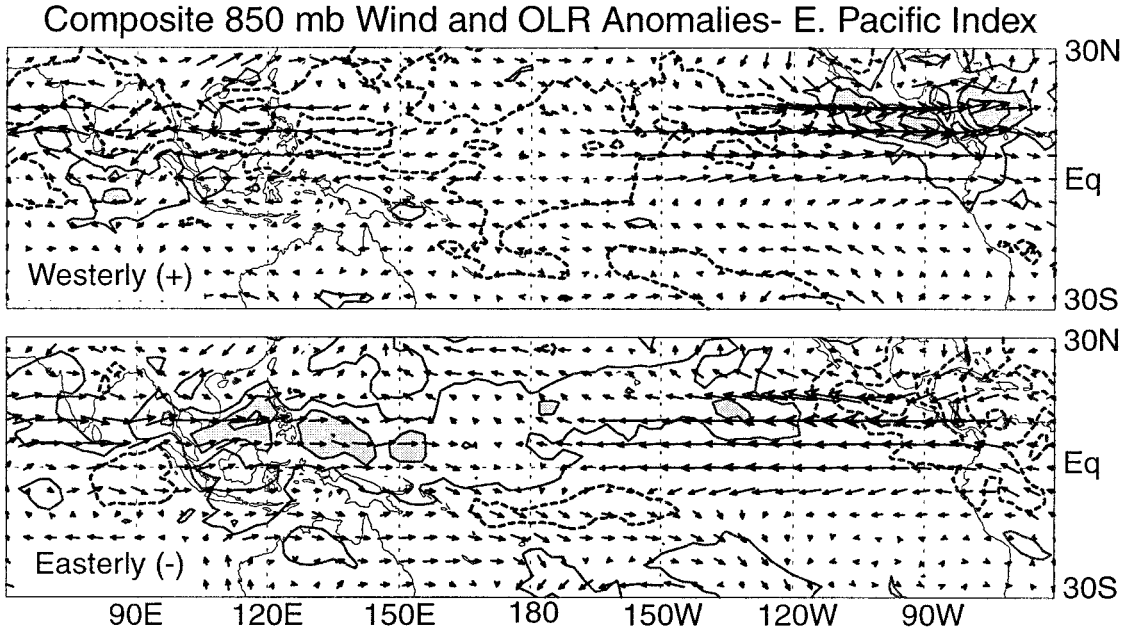

FIG. 4. Composite 850-mb wind anomalies and OLR anomalies for the top 20 positive and negative events. Contours are plotted every 10 W m^{-2} starting at 5 W m^{-2}. Positive OLR anomalies are dashed. OLR anomalies less than -15 W m^{-2} are shaded. Maximum wind vectors in the positive composite are 10.1 m s^{-1}.

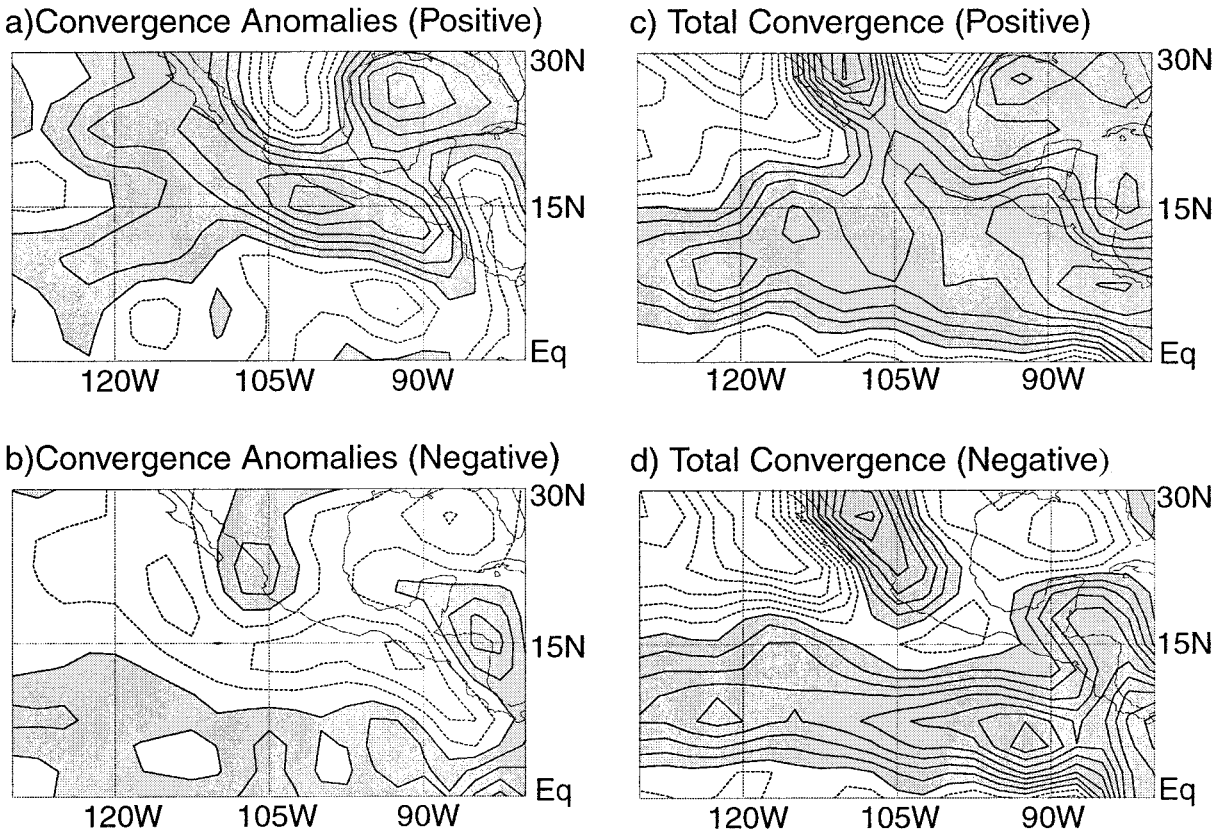

FIG. 5. 1000-mb convergence anomaly composites at lag 0 for the (a) top 20 positive and (b) top 20 negative events of the leading EOF for May–Nov 1979–97. The contour interval for the anomaly plots is 0.8×10^{-6} s^{-1}. 1000-mb total convergences (unfiltered) for the (c) top 20 positive and (d) top 20 negative events. The contour interval for the total field plots is 1.0×10^{-6} s^{-1}. Areas of convergence are shaded.

the date line, and out of phase with western Pacific and Indian Ocean wind variations, as is consistent with the MJO composites of MH00. The same analysis was also performed for 700-mb winds (not shown), and the structure of the leading EOF was similar to that at 850 mb. Previous studies have suggested that potential vorticity gradients at 700 mb might be important for hurricane genesis (Burpee 1972; Molinari et al. 1997). The amplitude of the MJO zonal wind variations over the eastern Pacific hurricane region is greater at 850 mb, however, so we used this level for our analysis.

The first principal component (PC) time series is derived by projecting the first EOF onto the zonal wind time series (annual cycle removed), including all seasons. The first PC is the amplitude of the first EOF. Variance of the PC time series peaks during August and September (Fig. 2). Convective heating near the eastern Pacific and Caribbean region during Northern Hemisphere (NH) summer likely contributes to the strength of the wind anomalies depicted by the first EOF.

A power spectrum of the PC time series indicates which frequencies dominate the EOF index. Fast Fourier transform analysis was performed on 18 segments of the PC time series (one segment per year). A Hanning window of length 64 pentads is used for a bandwidth of 0.0031 days^{-1}. The window is centered on August of each year to enable effective sampling of the summer hurricane season. The individual spectra are then averaged. The resulting spectrum has a statistically significant peak indicating a large amount of variance at periods between 30 and 60 days, periods characteristic of the MJO (Fig. 3). Spectral analysis using windows centered on February (not shown) indicates much less power at intraseasonal periods. Previous work showed that the MJO is strong in the east Pacific during summer (MH00), and the east Pacific zonal wind index that we use captures the intraseasonal variability in that region.

Comparison between the local eastern Pacific MJO index developed here and the global 850-mb zonal wind MJO index of MH00 indicates that they are closely related. The MH00 index was first developed by Maloney and Hartmann (1998) for studies of the global tropical MJO signal in all seasons. The zero lag correlation of the PC time series with the global MJO index of MH00 during May–November is -0.6 (not shown). This correlation is significant at the 95% level. A positive value of the MH00 index reflects westerly wind anomalies at 850 mb over the western Pacific and Indian

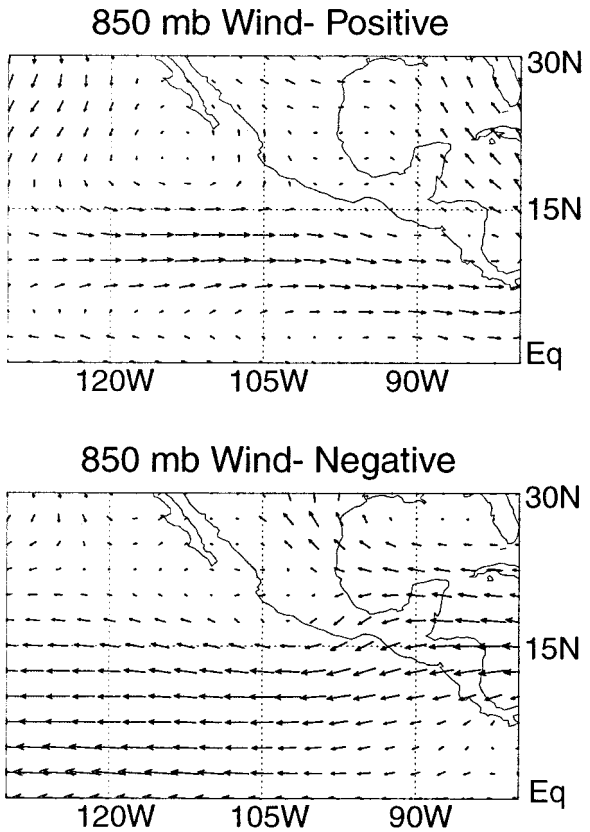

FIG. 6. 850-mb wind composites for the top 20 positive events and top 20 negative events of the leading EOF for May–Nov 1979–97. The magnitude of the largest wind vector in the positive composite is 8.1 m s^{-1}.

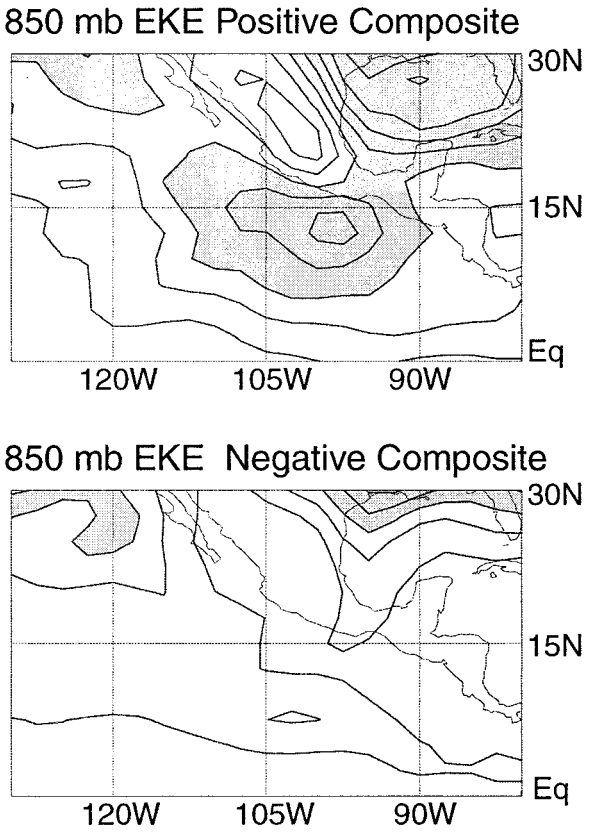

FIG. 7. Average 850-mb eddy kinetic energy for the (a) top 20 positive and (b) top 20 negative events. The contour interval is 2.0 (m^2 s^{-2}). Values greater than 8 (m^2 s^{-2}) are shaded.

Oceans and easterly wind anomalies in the east Pacific. When the amplitude of the leading east Pacific EOF is positive (strong westerly anomalies over the eastern Pacific), easterly anomalies occur over the western Pacific (Fig. 4). The intraseasonal mode in the east Pacific is thus closely connected with the global MJO as defined by the MH00 index. The eastern Pacific analysis in this paper was done with both the MJO index of MH00 and our east Pacific index. The composite fields are similar but stronger and more sharply defined with the east Pacific index. We present results only for the east Pacific index here. The strongest events as determined by the equatorial MH00 index do not necessarily coincide with the strongest eastern Pacific MJO events. The MJO is locally amplified by interaction with convection over the eastern Pacific during Northern Hemisphere summer. Eastern and western Pacific MJO variability is thus not perfectly correlated (just as Indian and western Pacific variability are not perfectly correlated). We therefore use a local MJO index in this paper to better focus on the interaction between local intraseasonal wind variations and local eddy development in the east Pacific.

The east Pacific MJO index is dominated by intraseasonal variations, and so it is not necessary to filter to remove interannual variability. Moreover, an index derived from filtered data is not as useful for real-time applications (as will be pursued in future work). Nonetheless, we have constructed the east Pacific MJO index using 80-day high-pass filtered data to double-check that interannual variability is not influencing the results of this paper. Results proved to be very similar to those derived from the unfiltered local index. MJO timescale variability clearly dominates our index, and interannual variability does not influence our conclusions. We have composited the east Pacific index on ENSO indices and found very little influence. This may be because ENSO has its strongest effect on SST near the equator, and the effect on intraseasonal variations at 10°N in the east Pacific is much weaker. Although variability at other than intraseasonal timescales may occasionally project onto the east Pacific index, the influence of this on our results is apparently very weak.

In summary, the leading EOF resembles the eastern Pacific zonal wind signal in the MJO composites of MH00, and the amplitude coefficient of this EOF varies on intraseasonal timescales of 30–60 days during NH summer. Intraseasonal zonal wind variations over the eastern Pacific during NH summer are significantly correlated at lags of around 15 days with those in the west-

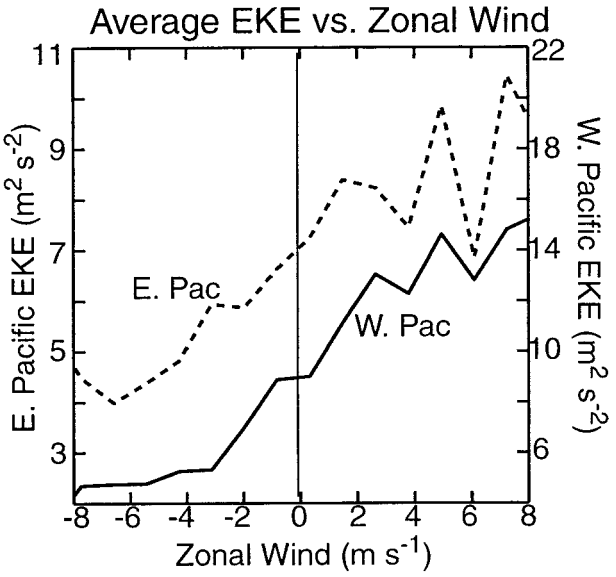

FIG. 8. Eastern Pacific (dashed) and western Pacific (solid) 850-mb eddy kinetic energy as a function of zonal wind during May–Nov 1979–97.

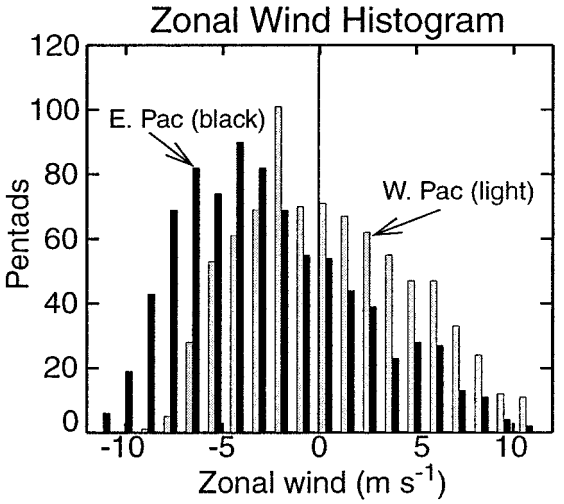

FIG. 9. Histogram of eastern Pacific (black) and western Pacific (light) zonal wind during May–Nov 1979–97.

ern Pacific (MH00). The structure of composite wind and OLR fields derived from the east Pacific EOF index also resemble the summertime MJO across the entire Pacific (Fig. 4). These results confirm the eastward propagation of the MJO signal from the western Pacific into the eastern Pacific noted in MH00.

b. Anomaly composites

Now we will examine wind *anomaly* composites associated with MJO variations over the eastern Pacific during NH summer. The top 20 positive and top 20 negative amplitude events of the leading EOF are determined for May–November from the PC time series. The 20 most extreme positive and negative events correspond to event amplitudes greater than 1.5 standard deviations from zero. These events are then averaged to produce positive and negative composite events. Composite fields get smaller with the inclusion of more events, as would be expected with a normally distributed statistic, but conclusions do not change. Figure 4 shows composites of OLR and 850-mb wind anomalies across the Pacific Ocean for the top positive and negative composite events. Strong westerly wind anomalies extend from the eastern Pacific into the western Caribbean Sea during westerly periods of the index. Wind anomalies over 10 m s^{-1} occur at the center of the westerly jet. Strong cyclonic shear occurs to the north of the jet core. Surface convergence accompanies this strong cyclonic shear (Fig. 5). Convergence at 850 mb (not shown) shows a similar spatial structure, but smaller magnitudes. Both the total convergence (annual cycle not removed) and the convergence anomalies are strong over the eastern Pacific hurricane formation region during

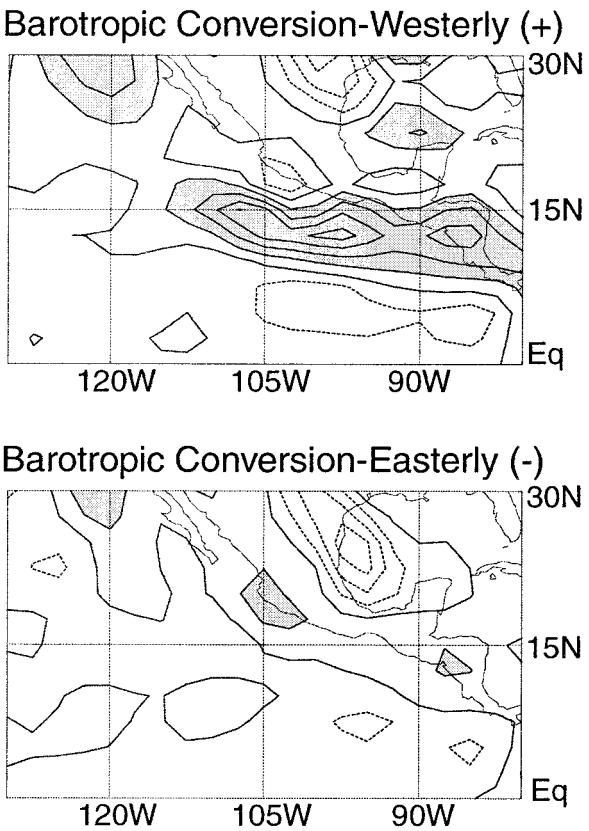

FIG. 10. The average time rate of change of eddy kinetic energy at 850-mb through barotropic conversion from the mean flow for the top 20 positive events and top 20 negative events during May–Nov 1979–97. Contour interval is 2.0×10^{-5} (m^2 s^{-2}) s^{-1}. Values greater than 2.0×10^{-5} (m^2 s^{-2}) s^{-1} are shaded.

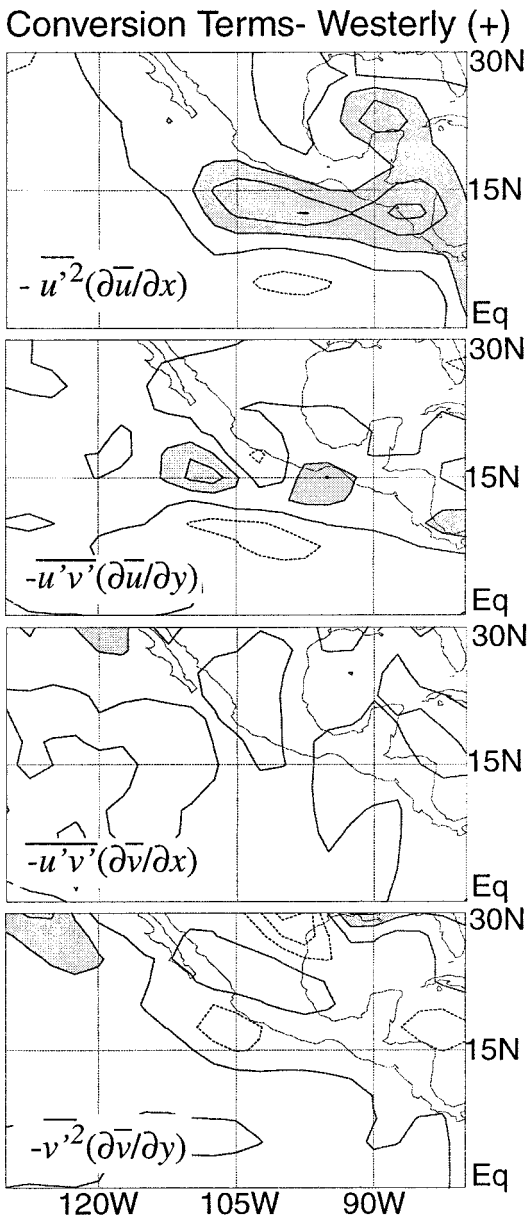

FIG. 11. Average 850-mb barotropic eddy kinetic energy conversion terms (a) $-\overline{u'^2}\partial\overline{u}/\partial x$, (b) $-\overline{u'v'}\partial\overline{u}/\partial y$, (c) $-\overline{u'v'}\partial\overline{v}/\partial x$, and (d) $-\overline{v'^2}\partial\overline{v}/\partial y$ for the top 20 positive events. Otherwise same as Fig. 10.

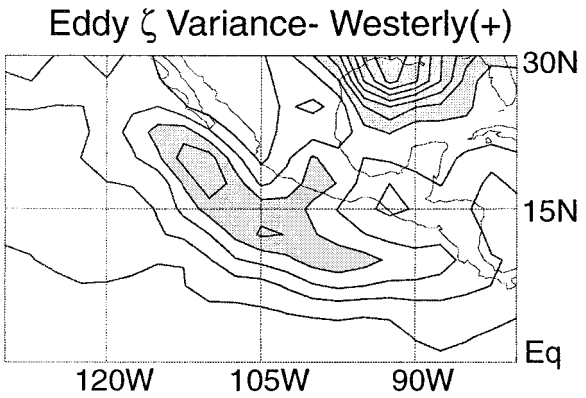

FIG. 12. 850-mb eddy vorticity variance for the positive composites. Contour interval is 4.0×10^{-11} s^{-2}. Values greater than 1.2×10^{-10} s^{-2} are shaded.

westerly events compared to easterly events. Convergence anomalies are highest in the regions of strong cyclonic shear. Cyclonic wind gyres, suggestive of Rossby waves forced by convection, occur to the north of the strongest wind anomalies. This forced response extends over the Gulf of Mexico, suggesting possible interactions with convection there through low surface pressure and low-level convergence (Fig. 5). Maloney and Hartmann (2000b) found a strong modulation of Gulf of Mexico tropical cyclones during eastern Pacific MJO westerly events. Strong easterly wind anomalies (about 4 m s^{-1}) are found over the western Pacific and Indian Oceans during eastern Pacific westerly phases, consistent with the boreal summer MJO composites of previous studies (e.g., Fig. 3 of MH00). Western Pacific MJO convection is similarly out of phase with eastern Pacific convection. Negative composites are similar to the positive composites, but with opposite signed anomalies.

c. *Total zonal wind field composites*

The *total* wind fields (as opposed to the anomaly fields) for the top positive and negative events are composited for use in assessing barotropic eddy kinetic energy generation. Figure 6 shows eastern Pacific 850-mb wind composites for positive and negative phases of the leading EOF at zero lag. A westerly jet over the eastern Pacific near 10°N is characteristic of positive phases with strong cyclonic shear of the zonal wind to the north of the jet core and strong anticyclonic shear to the south. The strong cyclonic shear, which coincides with the hurricane genesis region, is favorable for tropical cyclone development (Gray 1998). Surface convergence also occurs throughout the hurricane genesis region (Fig. 5). Potential vorticity analysis (not shown) indicates a reversal of the potential vorticity gradient on the north side of the cyclonic shear zone, a condition favorable for instability (Charney and Stern 1962). Potential vorticity reversals also extend with the westerly jet into the Caribbean Sea. Molinari et al. (1997) suggests that easterly waves may grow over the Caribbean and then move into the eastern Pacific where they contribute to hurricane formation. We will comment on this idea further in the next section.

Negative phases are characterized by strong easterly winds. An easterly zonal jet structure is present eastward of 100°W, with an anticyclonic shear zone prevailing to the west. In the negative phase anticyclonic wind shear and associated enhanced divergence occur in the region where tropical cyclones most often form, which would tend to inhibit cyclone development (Fig. 5). These pos-

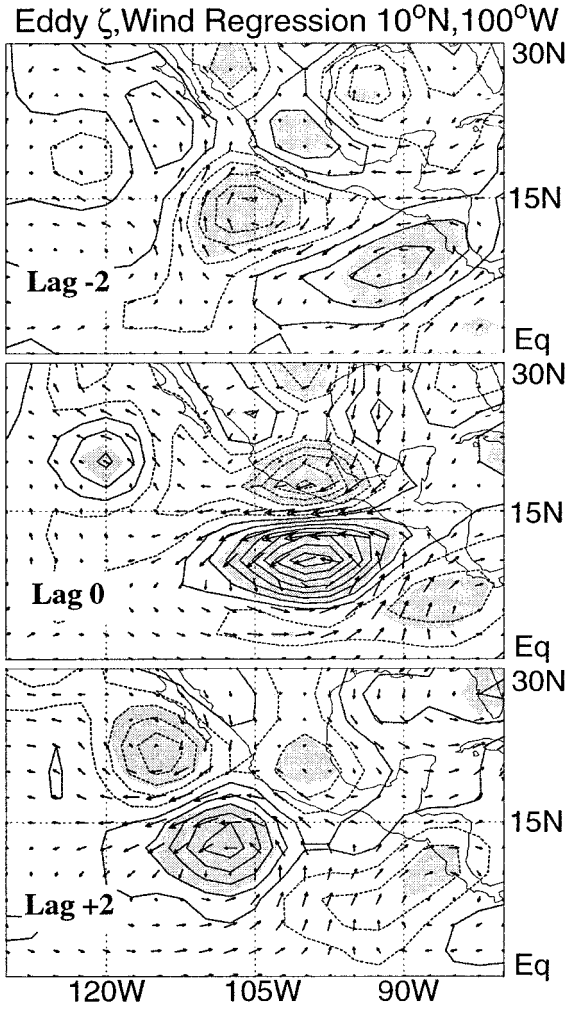

FIG. 13. Regression of eddy vorticity and eddy winds onto the eddy vorticity time series at 10°N, 100°W at lags of (a) −2, (b) 0, and (c) +2 days for the top 20 positive events. Contours are plotted every 1.6×10^{-6} s^{-1} starting at 0.8×10^{-6} s^{-1}. The maximum wind vector is 4.1 m s^{-1}. Vorticities significantly different from zero at the 95% level are shaded.

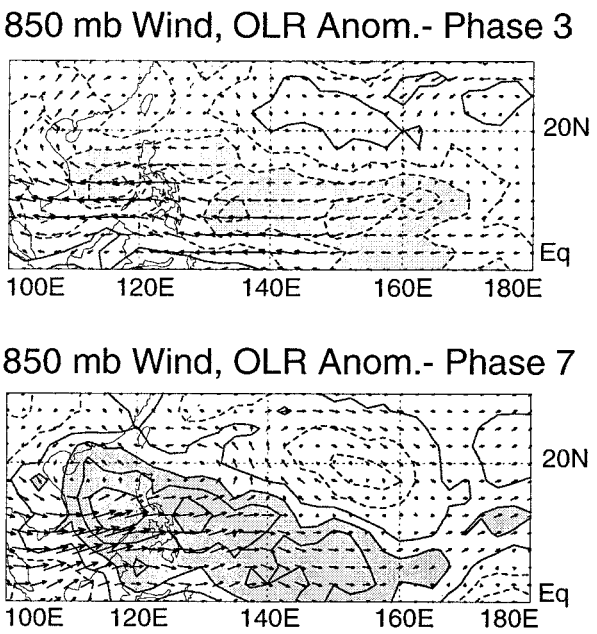

FIG. 14. Western Pacific phase 3 and phase 7 composite 850-mb wind and OLR anomalies for the top 20 MJO events. Contours are every 6 W m^{-2} starting at 3 W m^{-2}. Positive OLR anomalies are dashed. OLR anomalies less than −9 W m^{-2} are darkly shaded. OLR anomalies greater than 9 W m^{-2} are lightly shaded . Maximum wind vectors in the phase 7 composite are 6.3 m s^{-1}.

itive and negative composite wind fields are similar to the basic-state flows we will use in computing the barotropic energy conversions in section 3d.

We will show below that the westerly jet and associated wind convergence contribute to the growth of eddy disturbances through barotropic energy conversion. This leads to a concentration of eddy energy in the hurricane formation region. Strong cyclonic relative vorticity on the northern side of the westerly jet, surface convergence, and wave disturbances deriving energy from the mean flow create favorable conditions for tropical cyclone formation. Since cyclonic low-level eddies have been shown to be precursors to tropical cyclones (Zehr 1992), intensifying high wavenumber, low phase speed wave disturbances would be favorable for tropical cyclone formation. The concentration of eddy activity by the MJO may explain the tendency for tropical cyclones to cluster in time (Gray 1998). We will diagnose the structure and propagation characteristics of eddies deriving energy from the mean flow during westerly MJO periods.

d. Barotropic eddy–mean flow interactions

The barotropic energy conversion terms for eastern Pacific MJO westerly and easterly phases will now be presented. The momentum equations in pressure coordinates for a barotropic fluid, linearized about a basic state ($\overline{u}$, $\overline{v}$), can be approximated by

$$\frac{\partial}{\partial t}u' = -\overline{u}\frac{\partial}{\partial x}u' - u'\frac{\partial}{\partial x}\overline{u} - \overline{v}\frac{\partial}{\partial y}u' - v'\frac{\partial}{\partial y}\overline{u} - \frac{d\Phi'_a}{dx} + fv' - Du' \quad (1)$$

$$\frac{\partial}{\partial t}v' = -\overline{u}\frac{\partial}{\partial x}v' - u'\frac{\partial}{\partial x}\overline{v} - \overline{v}\frac{\partial}{\partial y}v' - v'\frac{\partial}{\partial y}\overline{v} - \frac{d\Phi'_a}{dy} - fu' - Dv', \quad (2)$$

where (u', v') are the eddy winds, Φ'_a is the part of the geopotential not in balance with the basic state flow, f is the Coriolis parameter, and D is the drag coefficient. The basic state flows ($\overline{u}$, $\overline{v}$) used in the energy calculations are defined as the composite anomaly winds (Fig.

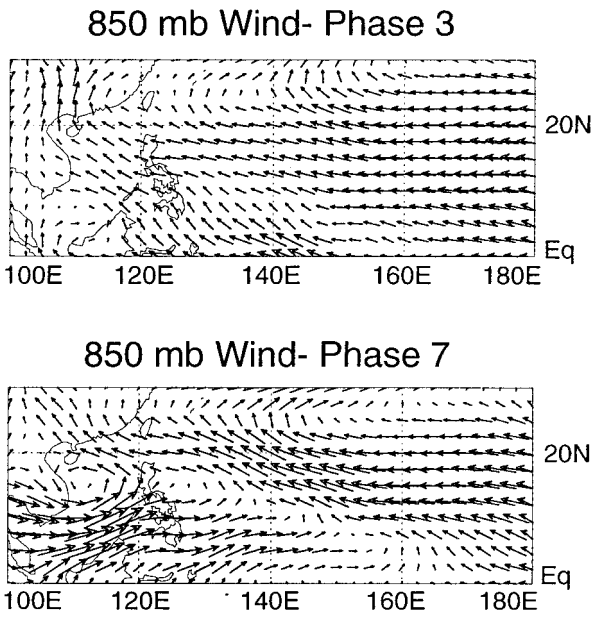

FIG. 15. Western Pacific total wind field for phases 3 and 7 of the top 20 MJO. Maximum wind vectors in the phase 7 composite are 9.7 m s^{-1}.

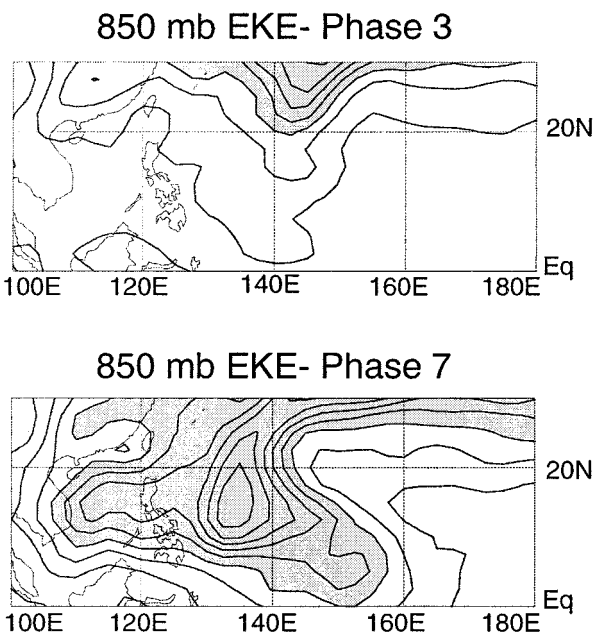

FIG. 16. Western Pacific average 850-mb eddy kinetic energy for phases 3 and 7 of the top 20 MJO events. The contour interval is 3.0 (m^2 s^{-2}). Values greater than 12.0 (m^2 s^{-2}) are shaded.

4), added to the annual cycle. Since two events may occur at different times of the year, their basic states may be slightly different. The basic-state flows for all events do not deviate greatly, however, from the composite flows displayed in Fig. 6. Results are nearly identical if the same basic state is used for all events. The basic-state flows vary slowly on MJO timescales. Eddy winds (u', v') are defined as the 20-day high-pass filtered daily (0000 UTC) wind values. High pass filtering ensures sufficient scale separation between the eddies and the intraseasonal flow variations in which they are embedded, but the results are not greatly different if unfiltered data are used to define the eddies.

To derive the tendency equation for eddy kinetic energy, we multiply (1) by u', (2) by v' and then add the resulting equations. After some simplification and ensemble averaging, the kinetic energy tendency can be written as

$$\frac{\partial}{\partial t}K' = -\overline{\mathbf{V}}\cdot\nabla K' - \overline{u'v'}\frac{\partial}{\partial y}\overline{u} - \overline{u'v'}\frac{\partial}{\partial x}\overline{v} - \overline{u'^2}\frac{\partial}{\partial x}\overline{u} - \overline{v'^2}\frac{\partial}{\partial y}\overline{v} - 2\mathrm{D}K' - (\overline{\mathbf{v}'\cdot\nabla\Phi'_a}), \quad (3)$$

where the eddy kinetic energy is given by

$$K' = \frac{1}{2}(\overline{u'^2} + \overline{v'^2}). \quad (4)$$

The first term on the rhs of (3) represents the advection of eddy energy by the mean flow, the next four terms are the barotropic conversion terms, $-2\mathrm{D}K'$ is the dissipation rate, and the last term is the work done by the eddy geopotential. For ease in reference, we will separate the barotropic conversion terms from the other contributions to the energy tendency,

$$\frac{\partial K'_{\mathrm{baro}}}{\partial t} = -\overline{u'v'}\frac{\partial}{\partial y}\overline{u} - \overline{u'v'}\frac{\partial}{\partial x}\overline{v} - \overline{u'^2}\frac{\partial}{\partial x}\overline{u} - \overline{v'^2}\frac{\partial}{\partial y}\overline{v}. \quad (5)$$

Figure 7 displays the average 850-mb eddy kinetic energy (EKE) for the top 20 positive (westerly phase) and negative (easterly phase) events. Positive composites indicate substantially higher EKE than the negative composites over the hurricane genesis region. EKE values are high across the hurricane genesis region in the positive composite, with values peaking at greater than 12 m^2 s^{-2}. EKE values over the genesis region for the negative composite are generally less than 4 m^2 s^{-2}. Interestingly, EKE is also enhanced over the Gulf of Mexico during the positive composites. Westerly eastern Pacific periods coincide with enhanced Gulf of Mexico hurricane activity (Maloney and Hartmann 2000b).

A companion paper uses a stochastically forced barotropic model to show that tropical EKE is enhanced during westerly wind regimes, particularly in the accumulation zone near the downstream end of westerly jets (Hartmann and Maloney 2001). Previous studies have also noted this relationship between tropical EKE and westerly winds (e.g., Arkin and Webster 1985; Webster and Chang 1988). Figure 8 plots 850-mb EKE as a function of zonal wind for the eastern Pacific Ocean. Eastern Pacific zonal wind and EKE are averaged over

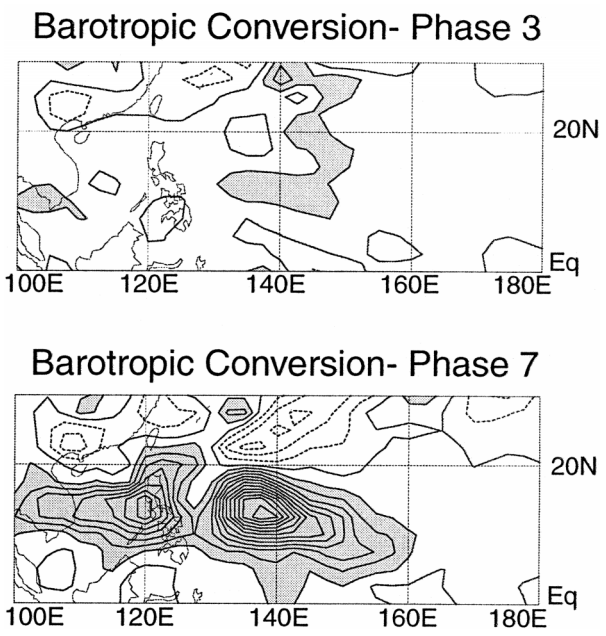

FIG. 17. Same as Fig. 10, but for the western Pacific during phase 3 and phase 7.

the region 7.5°–12.5°N, 102.5°–107.5°W, the region of maximum eastern Pacific zonal winds during MJO westerly events. Results are typical of relationships between zonal wind and EKE across the tropical eastern north Pacific. All pentads during May–November, not just pentads during MJO events, are used in this analysis. Pentads were organized by zonal wind values into bins of size 0.25 standard deviations (1.15 m s^{-1}). An average EKE and zonal wind was then computed for each bin. Although eastern Pacific zonal winds are easterly most of the time during the hurricane season (Fig. 9), EKE is considerably higher when eastern Pacific winds are westerly, consistent with the barotropic modeling results of Hartmann and Maloney (2001). Strong MJO events over the eastern Pacific can induce westerly winds, creating conditions that favor energetic eddies.

We hypothesize that small-scale, slow-moving eddies grow through barotropic energy conversion from the mean flow during MJO westerly jet periods over the eastern Pacific hurricane region. To test this hypothesis, we calculate the tendency of 850-mb EKE due to barotropic conversion for the positive and negative composites (Fig. 10). Strong generation of EKE occurs over the hurricane genesis region between 10° and 15°N in the positive composite. Generation rates peak near 0.8 $\times 10^{-4}$ (m^2 s^{-2}) s^{-1} near 12.5°N and 100°W. Ignoring dissipation, these generation rates can replace the observed westerly phase EKE in this region (12 m^2 s^{-2}; Fig. 7) in less than two days. Horizontal advection of EKE is small (not shown). Other generation maxima in the positive MJO composite occur over Central America and the Gulf of Mexico. Although not shown, generation rates over the Caribbean Sea are weak during the positive composite. Barotropic dynamics over the eastern Pacific may be sufficient to excite wave activity locally without the need for upstream wave growth over the Caribbean Sea. Upstream waves that do propagate into the eastern Pacific are likely intensified locally by barotropic conversion during MJO westerly periods. EKE generation in the hurricane region is rather weak in the negative composites as compared to the positive composites. Thus, barotropic wave growth tends to support

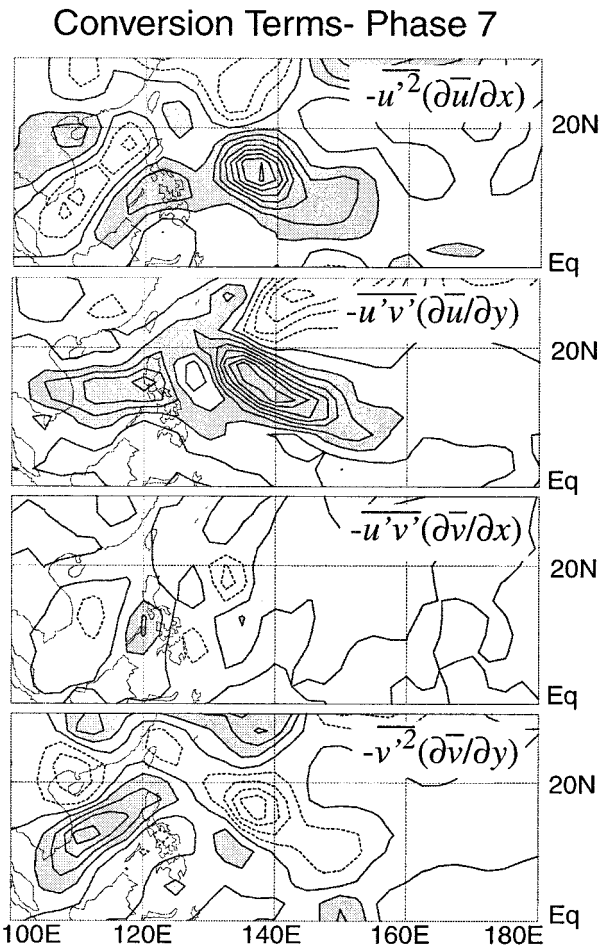

FIG. 18. Same as Fig. 11, but for the western Pacific during phase 7.

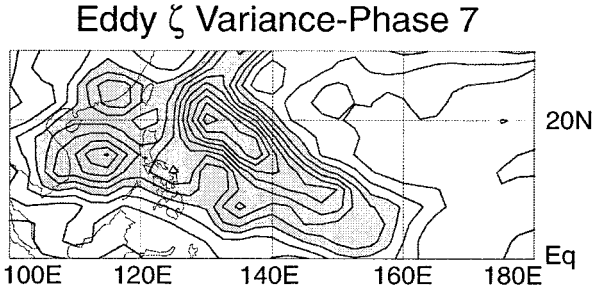

FIG. 19. Same as Fig. 12, but for the western Pacific during phase 7.

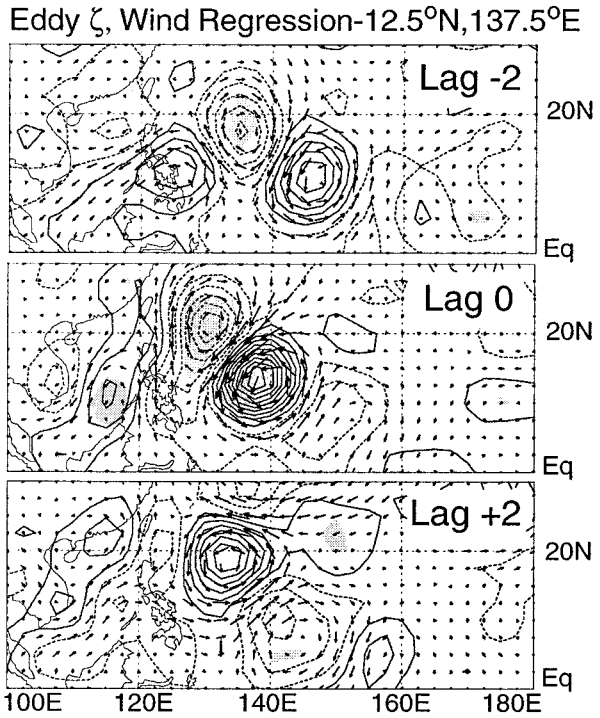

FIG. 20. Same as Fig. 13, but for the western Pacific during phase 7. The reference point is located at 12.5°N, 137.5°E. The maximum wind vector is 5.2 m s^{-1} at lag 0.

eastern tropical Pacific eddy activity during westerly MJO periods, but not during easterly MJO periods.

Figure 11 displays the contribution from each term in the barotropic EKE generation equation (5) for the positive composite. Generation is dominated by $-\overline{u'^2}\partial\overline{u}/\partial x$. Zonal variations in the MJO westerly jet over the eastern Pacific hurricane genesis region are of key importance in the barotropic generation of eddy kinetic energy. Generation by this term is consistent with barotropic wave accumulation, the importance of which has been noted in previous studies on the tropical circulation (e.g., Webster and Chang 1988; Sobel and Bretherton 1999). Eddy structure is dominated by zonal perturbations (see below). The $-\overline{u'^2}\partial\overline{u}/\partial x$ term also dominates generation over Central America and the Gulf of Mexico. The term $-\overline{u'v'}\partial\overline{u}/\partial y$ contributes some additional EKE generation over the hurricane genesis region. The dominant EKE generation, however, is caused by eddies interacting with longitudinal zonal wind gradients and not latitudinal gradients, contrary to the speculation in MH00.

The structure of the dominant eddies during MJO westerly events will be determined by regressing 850-mb eddy winds and vorticity onto the eddy vorticity at a location of high eddy vorticity variance. Eddy vorticity variance at 850 mb during the top 20 westerly events is shown in Fig. 12. Lying in the southern part of the hurricane genesis region, and within the region of high vorticity variance, we will use 10°N, 100°W as our principal point for examining eddy structure. Results are similar for other regression points in the near vicinity. Regressions of 850-mb eddy vorticity and 850-mb winds onto the 850-mb eddy vorticity time series at 10°N, 100°W are shown in Fig. 13 for the positive MJO phase. Regressions were computed at lags of -2 days, 0 days, and $+2$ days. Day 0 represents the time of maximum amplitude of the index for the top 20 westerly events. Amplitudes are scaled according to a positive 1 standard deviation value of eddy vorticity at the reference point. Shadings show vorticity values significantly different from zero at the 95% confidence level. Significance was determined using the *t* statistic, assuming 20 independent events.

Slow westward moving circulations centered at 10°N having scales of about 20° longitude and about 10° latitude dominate the composites. The strongest perturbations are found in zonal winds on the northern side of the eddies where rms wind perturbations in excess of 4.1 m s^{-1} can be found. Average movement is slowly westward at about 4.0 m s^{-1}. The eddies occur in regions of environmental low-level convergence (Fig. 5) and cyclonic shear. Therefore, slow-moving, small-scale eddies coincide with regions of low-level convergence and cyclonic environmental shear over the eastern Pacific hurricane region during westerly wind regimes associated with the MJO. Regression onto the vorticity time series at 20°N, 112°W produces structures that resemble tropical cyclones (not shown), and may explain the maximum of eddy vorticity variance in this region (J. Molinari 2000, personal communication).

4. Western Pacific energetics

Liebmann et al. (1994) noted a strong modulation of western Pacific tropical cyclones by the Madden–Julian oscillation. They found that western North Pacific tropical cyclones are about twice as likely during convectively active phases of the MJO than during suppressed phases. See Fig. 1 of Gray (1968) for a map of the western North Pacific tropical cyclone genesis region. We will use the MJO index of MH00 to determine westerly and easterly MJO phases over the western Pacific Ocean during May–November, and then do an energetics analysis similar to section 3. The MJO index of MH00 is constructed using the first two EOFs of the intraseasonal equatorial 850-mb zonal wind. For more details on the calculation of the MJO composites, see MH00. We will determine whether barotropic dynamics foster eddy growth over the western Pacific Ocean during westerly MJO periods. Phase 3 of the MJO life cycle represents the time of peak 850-mb easterly wind anomalies, suppressed convection, and suppressed tropical cyclone activity over the western Pacific. Phase 3 is the convectively suppressed MJO phase of Liebmann et al. (1994), when tropical cyclones are least likely. Phase 7 represents the time of peak westerly wind anomalies, enhanced convection, and enhanced tropical cyclone ac-

tivity. Phase 7 is the convectively active MJO phase of Liebmann et al. (1994), when tropical cyclones are most likely. Composite 850-mb wind and OLR anomalies for the top 20 MJO events during phases 3 and 7 are shown in Fig. 14, and total wind field composites are displayed in Fig. 15. The total wind field over the western Pacific Ocean is westerly during phase 7. The strongest westerly winds are located between 5°–10°N and 100°–140°E, and strong zonal wind convergence is evident to the east of the Philippines. Winds during phase 3 are generally easterly over the western Pacific.

Western north Pacific EKE for all NH summer pentads (not just MJO events) is generally higher during westerly periods than easterly periods (Fig. 8), similar to the eastern Pacific. Western Pacific EKE and zonal wind were averaged over the region 135°–140°E, 5°–10°N. Results are typical of relationships between zonal wind and EKE across the tropical western north Pacific. Average EKE at 850 mb during MJO phases 3 and 7 is shown in Fig. 16. Western Pacific EKE is considerably higher during phase 7 than phase 3, consistent with the tendency for higher EKE with westerly equatorial winds.

The heightened EKE during MJO westerly periods is supported by strong barotropic conversion (Fig. 17). The conversion is strong enough to replace the EKE maximum near 12.5°N, 132.5°E in a little over a day. Barotropic conversion during phase 3 is much weaker and not well organized. Lau and Lau (1992) found that barotropic conversion may provide a major energy source for western north Pacific summertime synoptic-scale disturbances. Our results show that this conversion process may be enhanced during MJO westerly periods. Conversion by the zonal convergence term $-\overline{u'^2}\partial\overline{u}/\partial x$ during MJO westerly phases at 850 mb is substantial (Fig. 18), consistent with the western Pacific MJO wave accumulation arguments of Sobel and Maloney (2000). This result is also consistent with the observation of Ritchie and Holland (1999) that regions of low-level confluence favor western Pacific tropical cyclone genesis. The $-\overline{u'v'}\partial\overline{u}/\partial y$ term, however, produces EKE generation comparable to the $-\overline{u'^2}\partial\overline{u}/\partial x$ term. Maximum generation with the term $-\overline{u'v'}\partial\overline{u}/\partial y$ is coincident with cyclonic shear of the basic-state zonal wind. The north side of this shear zone may contain potential vorticity gradient reversals that support barotropic instability (Molinari et al. 1997), although future work is necessary to confirm this relationship. The term $-\overline{v'^2}\partial\overline{v}/\partial y$ provides significant contributions to generation near 110°E.

Eddy 850-mb winds and vorticity during phase 7 are regressed onto the eddy vorticity at 12.5°N, 137.5°E (Fig. 20), which is within the region of highest eddy vorticity variance (Fig. 19) and highest phase 7 EKE (Fig. 16). Results are similar for other regression points in the near vicinity. Small-scale, slow-moving eddies are characteristic of MJO westerly periods. The eddies move northwestward at about 3° longitude and 2° latitude per day (about 4.5 m s^{-1}), comparable to the eddy propagation during westerly MJO phases over the eastern Pacific. Western Pacific eddies are not as zonally elongated as their eastern Pacific counterparts, however. Maximum rms eddy wind speeds are 5.2 m s^{-1}.

The western Pacific results indicate that small-scale, slow-moving eddies grow through barotropic conversion from the mean flow during westerly MJO periods. Eddies deriving energy from the mean flow can provide seed disturbances for tropical cyclone formation during MJO westerly periods. They occur in regions of cyclonic mean low-level shear and warm mean sea surface temperatures that favor further growth by accessing the energy available in latent heat.

5. Conclusions

The goal of this investigation was to examine the influence of low-level barotropic dynamics on tropical Pacific eddy disturbances during Madden–Julian oscillation (MJO) events. Periods of strong 850-mb anomalous westerlies and easterlies are typical of opposite phases of the MJO over the tropical eastern and western North Pacific Ocean during Northern Hemisphere summer. When intraseasonal 850-mb wind anomalies associated with the MJO are westerly, eddy kinetic energy (EKE) is generated due to barotropic conversion from the mean low-level flow. Energetic eddies may provide seed disturbances for tropical cyclones.

Empirical orthogonal function analysis on eastern Pacific 850-mb zonal winds was used to locally diagnose the top 20 events for easterly and westerly MJO wind regimes. Small-scale, slow-moving, energetic eddies grow during periods of strong MJO westerly jets through barotropic EKE conversion from the mean flow. These growing eddies, in conjunction with warm mean sea surface temperatures, strong surface convergence, and 850-mb cyclonic shear, create conditions favorable for tropical cyclone and hurricane formation. MJO westerly periods foster similar eddy–mean flow interactions over the western Pacific, where Liebmann et al. (1994) demonstrated a strong modulation of tropical cyclones by the MJO.

The barotropic conversion term $-\overline{u'^2}\partial\overline{u}/\partial x$ is important for barotropic EKE conversion during MJO westerly periods in both the east and west Pacific, indicating the importance of zonal variations in the zonal wind for eddy growth. This mechanism is consistent with barotropic wave accumulation by a mean convergent zonal flow (Sobel and Bretherton 1999). Barotropic conversion over the eastern Pacific is dominated by $-\overline{u'^2}\partial\overline{u}/\partial x$ during MJO westerly periods. The conversion term $-\overline{u'v'}\partial\overline{u}/\partial y$ contributes some amplitude to the total generation over the eastern Pacific, but generally plays a secondary role. The term $-\overline{u'v'}\partial\overline{u}/\partial y$ is of comparable magnitude to $-\overline{u'^2}\partial\overline{u}/\partial x$ over the western Pacific, however. Periods of strong MJO easterlies are characterized by lesser EKE and negligible eddy generation by bar-

otropic conversion in both the east and west Pacific. Anomalous low-level divergence and anticyclonic vorticity also occur during easterly phases, making conditions unfavorable for tropical cyclone genesis. In part II of this study Hartmann and Maloney (2001) use a stochastic 2D barotropic model to determine the characteristics of eddies that most efficiently derive energy from the MJO westerly and easterly basic states. Model eddy characteristics and their relation to intraseasonal flow anomalies prove to be similar to those observed.

Previous work has suggested the importance of upstream growth of eddies over the Caribbean Sea for eastern Pacific tropical cyclone formation (e.g., Molinari et al. 1997). Our results indicate that energetics local to the eastern Pacific may be sufficient to foster cyclone formation, especially during MJO westerly wind periods. Maloney and Hartmann (2000a) emphasized, however, that not all eastern Pacific hurricanes are modulated by the MJO. Growth of wave disturbances over the Caribbean may therefore be important for eastern Pacific hurricane formation during certain weather regimes, and we have not considered baroclinic effects. Our results also do not directly contradict theories for eastern Pacific cyclone formation based on orographically induced circulations (Zehnder 1991; Mozer and Zehnder 1996). Eddies produced by orography may grow through eddy–mean flow interactions during MJO westerly or easterly periods. Reduction or reversal of the prevailing easterlies impinging on the terrain of Central America and Mexico during westerly MJO periods may significantly alter the effect of orography. Case studies of tropical cyclone genesis during MJO westerly periods may help to elucidate some of these issues.

Acknowledgments. The authors would like to thank George Kiladis, John Molinari, Adrian Matthews, and one anonymous reviewer for their constructive criticism. This work was supported by the Climate Dynamics Program of the National Science Foundation under Grant ATM-9873691.

REFERENCES

Arkin, P., and P. J. Webster, 1985: Annual and interannual variability of the tropical–extratropical interaction: An empirical study. *Mon. Wea. Rev.,* **113,** 1510–1523.

Burpee, R. W., 1972: The origin and structure of easterly waves in the lower troposphere of North Africa. *J. Atmos. Sci.,* **29,** 77–90.

Charney, J. G., and M. E. Stern, 1962: On the stability of internal baroclinic jets in a rotating atmosphere. *J. Atmos. Sci.,* **19,** 159–172.

Davidson, N. E., and H. H. Hendon, 1989: Downstream development in the Southern Hemisphere monsoon during FGGE/WMONEX. *Mon. Wea. Rev.,* **117,** 1458–1470.

Dickinson, M. J., 2000: Mixed Rossby-gravity waves and western Pacific tropical cyclogenesis. Preprints, *24th Conf. on Hurricanes and Tropical Meteorology,* Ft. Lauderdale, FL, Amer. Meteor. Soc., 266–267.

Emanuel, K. A., 1988: Maximum intensity of hurricanes. *J. Atmos. Sci.,* **45,** 1143–1155.

Gray, W. M., 1968: Global view of the origin of tropical disturbances and storms. *Mon. Wea. Rev.,* **96,** 669–697.

———, 1998: The formation of tropical cyclones. *Meteor. Atmos. Phys.,* **67,** 37–69.

Gruber, A., and A. F. Krueger, 1984: The status of the NOAA outgoing longwave radiation data set. *Bull. Amer. Meteor. Soc.,* **65,** 958–962.

Hartmann, D. L., and E. D. Maloney, 2001: The Madden–Julian oscillation, barotropic dynamics, and North Pacific tropical cyclone formation. Part II: Stochastic barotropic modeling. *J. Atmos. Sci.* **58,** 2559–2572.

Holland, G. J., 1995: Scale interaction in the western Pacific monsoon. *Meteor. Atmos. Phys.,* **56,** 57–79.

Hoskins, B. J., I. N. James, and G. H. White, 1983: The shape, propagation, and mean-flow interaction of large-scale weather systems. *J. Atmos. Sci.,* **40,** 1595–1612.

Kalnay, E., and Coauthors, 1996: The NCEP/NCAR 40-Year Reanalysis Project. *Bull. Amer. Meteor. Soc.,* **77,** 437–471.

Lau, K.-H., and N.-C. Lau, 1992: The energetics and propagation dynamics of tropical summertime synoptic-scale disturbances. *Mon. Wea. Rev.,* **120,** 2523–2539.

Liebmann, B., H. H. Hendon, and J. D. Glick, 1994: The relationship between tropical cyclones of the western Pacific and Indian Oceans and the Madden–Julian oscillation. *J. Meteor. Soc. Japan,* **72,** 401–411.

Madden, R. A., and P. R. Julian, 1994: Observations of the 40–50-day tropical oscillation—A review. *Mon. Wea. Rev.,* **122,** 814–837.

Mak, M., and M. Cai, 1989: Local barotropic instability. *J. Atmos. Sci.,* **46,** 3289–3311.

Maloney, E. D., and D. L. Hartmann, 1998: Frictional moisture convergence in a composite life-cycle of the Madden–Julian oscillation. *J. Climate,* **11,** 2387–2403.

——, and ——, 2000a: Modulation of eastern North Pacific hurricanes by the Madden–Julian oscillation. *J. Climate,* **13,** 1451–1460.

——, and ——, 2000b: Modulation of hurricane activity in the Gulf of Mexico by the Madden–Julian Oscillation. *Science,* **287,** 2002–2004.

Molinari, J., and D. Vollaro, 2000: Planetary and synoptic-scale influences on eastern Pacific tropical cyclogenesis. *Mon. Wea. Rev.,* **128,** 3296–3307.

——, D. Knight, M. Dickinson, D. Vollaro, and S. Skubis, 1997: Potential vorticity, easterly waves, and eastern Pacific tropical cyclogenesis. *Mon. Wea. Rev.,* **125,** 2699–2708.

Montgomery, M. T., and B. F. Farrell, 1993: Tropical cyclone formation. *J. Atmos. Sci.,* **50,** 285–310.

Mozer, J. B., and J. A. Zehnder, 1996: Lee vorticity production by large-scale tropical mountain ranges. Part I: A mechanism for tropical cyclogenesis in the eastern North Pacific. *J. Atmos. Sci.,* **53,** 521–538.

Nieto Ferreira, R., and W. H. Schubert, 1997: Barotropic aspects of ITCZ breakdown. *J. Atmos. Sci.,* **54,** 261–285.

Norquist, D. C., E. E. Recker, and R. J. Reed, 1977: The energetics of African wave disturbances as observed during phase III of GATE. *Mon. Wea. Rev.,* **105,** 334–342.

North, G. R., T. L. Bell, R. F. Cahalan, and F. J. Moeng, 1982: Sampling errors in the estimation of empirical orthogonal functions. *Mon. Wea. Rev.,* **110,** 699–706.

Ritchie, E. A., and G. J. Holland, 1999: Large-scale patterns associated with tropical cyclogenesis in the western Pacific. *Mon. Wea. Rev.,* **127,** 2027–2043.

Schubert, W. H., P. E. Ciesielski, D. E. Stevens, and H. Kuo, 1991: Potential vorticity modeling of the ITCZ and the Hadley circulation. *J. Atmos. Sci.,* **48,** 1493–1509.

Shapiro, L. J., 1978: The vorticity budget of a composite African tropical wave disturbance. *Mon. Wea. Rev.,* **106,** 806–817.

Sobel, A. H., and C. S. Bretherton, 1999: Development of synoptic-scale disturbances over the summertime tropical northwest Pacific. *J. Atmos. Sci.,* **56,** 3106–3127.

——, and E. D. Maloney, 2000: Effect of ENSO and the MJO on western north Pacific tropical cyclones. *Geophys. Res. Lett.,* **27,** 1739–1742.

Thorncroft, C. D., and B. J. Hoskins, 1994a: An idealized study of African easterly waves. I: A linear view. *Quart. J. Roy. Meteor. Soc.,* **120,** 953–982.

——, and ——, 1994b: An idealized study of African easterly waves. II: A nonlinear view. *Quart. J. Roy. Meteor. Soc.,* **120,** 983–1015.

Webster, P. J., and H.-R. Chang, 1988: Equatorial energy accumulation and emanation regions: Impacts of a zonally varying basic state. *J. Atmos. Sci.,* **45,** 803–829.

Zehnder, J. A., 1991: The interaction of planetary-scale tropical easterly waves with topography: A mechanism for the initiation of tropical cyclones. *J. Atmos. Sci.,* **48,** 1217–1230.

Zehr, R. M., 1992: Tropical cyclogenesis in the western North Pacific. NOAA Tech. Rep. NESDIS 61, 181 pp. [Available from U.S. Department of Commerce, NOAA/NESDIS, 5200 Auth Rd., Washington, DC 20233.]